Journal of Energy Storage 72 (2023) 108479

Contents lists available at ScienceDirect

Journal of Energy Storage

journal homepage: www.elsevier.com/locate/est

Research Papers

Edge-based solution for battery energy management system: Investigating the integration capability into the building automation system

Mustapha Habib [a,*], Elmar Bollin [b], Qian Wang [a,c]

[a] Division of Building Technology and Design, KTH Royal Institute of Technology, Department of Civil and Architectural Engineering, 11428 Stockholm, Sweden
[b] Institute of Energy System Technology, Offenburg University of Applied Sciences, 77652 Offenburg, Germany
[c] Uponor AB, Hackstavägen 1, 721 32 Västerås, Sweden

ARTICLE INFO

Keywords:
Photovoltaics
Battery energy management system
Edge control
Building automation system

ABSTRACT

Recently, photovoltaic (PV) with energy storage systems (ESS) have been widely adopted in buildings to overcome growing power demands and earn financial benefits. The overall energy cost can be optimized by combining a well-sized hybrid PV/ESS system with an efficient energy management system (EMS). Generally, EMS is implemented within the overall functions of the Building Automation System (BAS). However, due to its limited computing resources, BAS cannot handle complex algorithms that aim to optimize energy use in real-time under different operating conditions. Furthermore, islanding the building's local network to maximize the PV energy share represents a challenging task due to the potential technical risks. In this context, this article addresses an improved approach based on upgrading the BAS data analytics capability by means of an edge computing technology. The edge communicates with the BAS low-level controller using a serial communication protocol. Taking advantage of the high computing ability of the edge device, an optimization-based EMS of the PV/ESS hybrid system is implemented. Different testing scenarios have been carried out on a real prototype with different weather conditions, and the results show the implementation feasibility and technical performance of such advanced EMS for the management of building energy resources. It has also been proven to be feasible and advantageous to operate the local energy network in island mode while ensuring system safety. Additionally, an estimated energy saving improvement of 6.23 % has been achieved using optimization-based EMS compared to the classical rule-based EMS, with better ESS constraints fulfillment.

1. Introduction

The acceleration of the electrification process in energy sectors has led to an increase in electricity consumption of about 2.5 % per year. The current global electricity use in the building sector is around 30 % of the total final energy usage and consists of approximately 55 % of the global electricity demand [1,2]. Up to date, solar photovoltaics (PV) is one of the most mature and widely used renewable energy sources in buildings [3,4]. However, PV systems are highly intermittent and dependent on climatic conditions, thereby, they heavily rely on electric storage systems (ESS). One of the most commonly used ESS technologies in buildings is electro-chemical batteries. However, it may have significant impacts on how the energy management system (EMS) should be integrated to achieve optimal system-level performance [5]. Typically, EMS is implemented within building automation systems (BASs), using low-level controllers such as programmable logic controllers (PLCs).

BAS is a data acquisition and control system that incorporates various functionalities provided by the control system of a building [6]. Such functionalities cover, e.g., temperature and air quality monitoring, lighting system control, heating, ventilation, and air conditioning (HVAC) system control, electricity control, access control, security control, fire control, sending signals when faults occur, etc. [7]. BASs are computer-based automated systems, rely on sensors to collect the condition or status of control parameters, actuators to conduct physical actions, and communication and interoperability to optimize the overall energy optimization via BAS. Different subsystems in the BAS and devices manufactured by various vendors need to communicate with each other. As mentioned, data communication protocols play key roles in information exchange in the BAS domain. Recent protocols, such as Building Automation and Control Networks (BACnet) and MODBUS, dominate BAS communication networks [6]. However, BAS has some limitations, related mainly to its design: real-time data availability, computing capability, and big data analysis and storage are among

* Corresponding author.
E-mail addresses: mushab@kth.se (M. Habib), bollin@hs-offenburg.de (E. Bollin), qianwang@kth.se (Q. Wang).

https://doi.org/10.1016/j.est.2023.108479
Received 15 March 2023; Received in revised form 27 June 2023; Accepted 21 July 2023
Available online 28 July 2023

Symbols and abbreviations

BACnet	Building automation and control networks
BAS	Building automation system
BIM	Building information modeling
BSP	Battery status processor
DOD	Depth of discharge
EMS	Energy management system
ESS	Energy storage systems
GA	Genetic algorithms
HMI	Human machine interface
HVAC	Heating, ventilation and air conditioning
INES	Institute of energy systems technologies
IoT	Internet of things
ML	Machine learning
MPPT	Maximum power point tracking
OPC UA	Open platform communications united architecture
OS	Operation system
PC	Personal computer
PCC	Point of common coupling
PLC	Programmable logic controller
PV	Photovoltaic
RCC	Remote control center
RTOS	Real time operation system
SOC	State of charge
SOC_{MIN}	Minimum allowed limit of batteries state of charge
SOC_{MAX}	Maximum allowed limit of batteries state of charge
SQL	Structured query language
P_{PV}	Supplied power from PV system [kW]
V_B	Batteries voltage [V]
I_B	Batteries current [A]
P_g	Exchanged power with the grid [kW]
α	Grid relay state
η_{PV}	Power conversion efficiency from photovoltaic systems
η_B	Power conversion efficiency from batteries
C	Batteries capacity [Ah]
P_{load}	Load power [kW]
X_1	Decision variable 1 (grid relay)
X_2	Decision variable 2 (batteries current setpoint) [A]
$P_{ESS-MAX}$	Maximum power allowed by the converter [kW]
K_i	Weighting coefficient
E_{PV}	Supplied photovoltaic energy [kWh]
E_{load}	Energy demand [kWh]
E_{grid}	Energy exchanged with the grid utility [kWh]

them. Additionally, current BASs fail to offer real-time data processing [8].

To enhance data analytics for BASs, some literature discusses the advantage of introducing a cloud-based computing paradigm, this arrangement transfers collected sensor data to the cloud, where machine learning (ML) is harnessed to generalize overall system behavior [9]. In terms of validated use cases in this context, an internet of things (IoT)-enabled building EMS is developed, and its stability and robustness are confirmed [10]. A real-time digital model of an office building is created by analyzing building information modeling (BIM) and data collected from an IoT-enabled sensor network [11]. It has been verified that the cloud-based computing paradigm can achieve energy savings of up to 20 % on HVAC installed in an experimental building [12]. Even though BAS-Cloud offers such big data processing capability with increasing quantities of heterogeneous building data, it is challenging for the paradigm to achieve real-time results. In addition, other critical issues have not been addressed, such as communication overhead, network congestion [13], privacy, and data leaks [14].

Alternatively, instead of using BAS-Cloud solutions, use a distributed computing paradigm, namely, BAS-Edge, that brings data computing, storage, and network functions closer to end-users on site. Edge computing has been an emerging solution in various fields [15]. This is mainly due to a few advantages observed during the implementation of alternative BAS solutions:

- A data processing scheme that utilizes collaborative edges located near user sites for information sharing, aiming at reducing the amount of data transmitted to the cloud while improving data analytics.
- BAS-Edge covers cyber-security concerns by processing private information via edges located in or near buildings as much as possible.
- There are considerable computing and storage resources that can solve the issue of real-time data analytics.

The intermittent and unpredictable behavior of PV systems may lead to harmful operation scenarios for eventual connected ESS; this matter becomes crucial when the building microgrid is islanded [16,17]. The challenge of such operations is the impact of a sudden imbalance between load and power generation; any implemented control mechanism has to ensure that such imbalances become controllable by the grid-forming unit [18]. As the frequency in microgrids is an indirect indicator of the power balance, it can be used as a control signal without the need for additional communications. In this regard, any connected ESS inverters are intended to reduce their power outputs when the microgrid frequency exceeds a certain level (e.g., 50.2 Hz) [19]. This kind of frequency control approach can not only be used as a grid support mode for ESS but can also perform energy management to control the ESS state of charge (SOC) [20]. A similar approach is validated in [21] using fuzzy-controlled PV/ESS inverters, in which, the goal is to simultaneously perform battery energy management and frequency regulation support. Predictive EMS approaches may also provide some potential solutions to deal with ESS operation in a hybrid energy system with a fluctuating power balance. In this context, authors in [22] propose a 24-hour predictive management of a hybrid energy system of a residential building, in which, the battery lifetime increase is targeted. However, the proposed EMS performance is highly related to weather forecast accuracy, which is still a working topic up to date [23], and the island operation mode use case is excluded. All the mentioned EMS approaches are designed for one microgrid operation mode. The adoption of the new operation conditions associated with the change in operation modes (from island to grid-connected and vice versa) is not considered. This leads to the need for an optimization-based EMS, that takes into account microgrid operation modes. Typically, in the framework of BAS, ESS's current setpoint is to be defined by a PLC code in real-time. However, as mentioned previously, PLC does not support EMS approaches requiring high computing power. Additionally, IEC 61131-3, which is the reference standard for PLC programming, makes it a challenging task to implement complex EMS algorithms.

This article addresses and validates an optimization-based EMS as a high-level energy manager. The proposed method simultaneously integrates frequency regulation support and battery management in both microgrid operation modes. To overcome the limitations associated with the PLC computing capability, advanced edge hardware is used instead, the proposed EMS approach is accomplished based on successful communication between the edge and BAS. The remainder of this paper is organized into three sections: Section 2 describes the proposed optimization-based EMS method. In Section 3, more details of the experimental validation setup are given, while Section 4 will be the

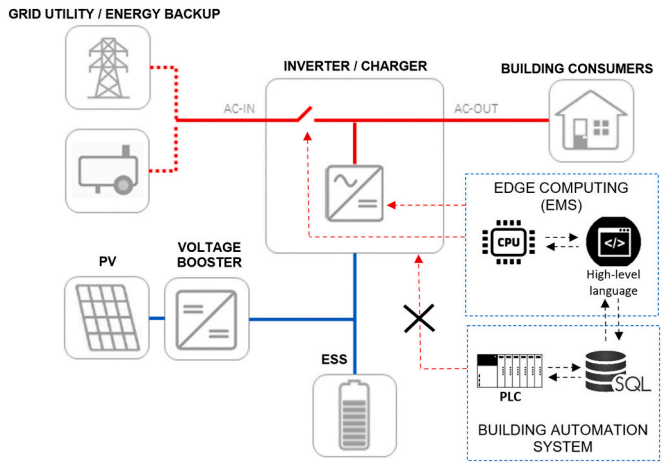

Fig. 1. Proposed EMS validation strategy during test phase.

stage for some results and discussions.

2. Method description

The proposed energy manager algorithm is based on continuously performing an optimization task each control cycle by taking new measurement data each time. The optimization outcomes are the ESS current setpoint to be applied during the next cycling time and the state of the relay connecting the hybrid system to the grid utility. Those optimal setpoints are designed to minimize the use of imported energy from the grid while optimally supervising ESS SOC in both operation modes: islanded and grid-connected. It is worth mentioning that in island mode, the ESS inverter switches from current source mode to voltage source mode, in which it oversees on providing voltage and frequency to the whole microgrid. Both PV and ESS inverters reduce their power outputs proportionally with frequency increases. However, regardless of the power curtailment option, the PV inverter cannot be controlled by the proposed energy manager, in which, the Maximum Power Point Tracking (MPPT) algorithm is the only active control. During method validation, BAS is bypassed temporarily by the edge energy monitoring device as Fig. 1 shows. With this control procedure, the ESS inverter/charger is monitored solely by the edge device. For this end, data is being fetched from the BAS database cyclically before running the optimization. Thanks to its high computing capability, the edge energy manager can host compilers for high-level programming languages needed for complex EMS implementation.

2.1. Power flow equation

The power balance equation of the hybrid energy system is formulated as below:

$$P_{load} = \eta_{PV} P_{PV} + \eta_B V_B I_B + \alpha \bullet P_g \tag{1}$$

with P_{PV} is the supplied power from PV system; V_B and I_B are the batteries bank voltage and current respectively; P_g is the exchanged grid power, it takes positive values during energy importation from the grid utility and negative values when feeding back energy to the grid utility; α is the grid relay: it takes the value "1" in grid-connected mode and "0" in island mode; η_{PV} and η_B are the energetic efficiency of PV and the batteries inverter/charger respectively including the cables power waste.

2.2. Battery state of charge equation

ESS SOC is a key parameter that should be supervised continuously, it is determined via the equation formulated below:

$$SOC(t+\Delta T) = SOC(t) - 100 \bullet \frac{I_B.\Delta T}{C} \tag{2}$$

wherein, $SOC(t)$ is actual battery SOC at time t; $SOC(t + \Delta T)$ is the predicted SOC with prediction horizon ΔT; C is the battery nominal capacity and I_B is the battery charge/discharge current which is obtained using Eq. (3).

$$I_B = P_B / V_B \tag{3}$$

In order to reduce the algorithm complexity, V_B is chosen to be constant (48 V) during all operation conditions.

2.3. Cost function

The cost function for optimization is formulated by combining three weighted terms:

$$J = K_1 X_1 (P_{load} - P_{PV} - \eta_B V_B X_2) + K_2 (1 - X_1)(P_{PV} + \eta_B V_B X_2 - P_{load})^2 + K_3 X_1 \tag{4}$$

where, X_1 is the state of the grid relay (Boolean variable); X_2 is ESS current setpoint. It is worthy to note that when the grid relay is off, ESS is uncontrollable since it works as an energy buffer depending on the power balance in the building local network. In this situation, X_2 is the predicted ESS current that will be used to estimate SOC; K_1, K_2 and K_3 are weighting coefficients.

The optimizer manipulates two variables to minimize J which are X_1 and X_2 respecting to the following functioning constraints:

$$-P_{ESS-MAX} \le \eta_B X_2 V_B \le P_{ESS-MAX} \tag{5}$$

$$SOC_{MIN} \le SOC(t) - 100 \bullet \frac{X_2 \Delta T}{C} \le SOC_{MAX} \tag{6}$$

where $P_{ESS-MAX}$ is the maximum allowed power to be exchanged through the inverter/charger; SOC_{MIN} and SOC_{MAX} are respectively the minimum and maximum predefined limits for ESS SOC.

The cost function is composed of two main terms, in which only one is active in a particular operation mode:

Term 1 ($X_1 = 1$): when the constraints, formulated in Eqs. (5) and (6), are expected to be violated in the next cycling time, the energy manager connects the local network to the grid and uses the grid as a backup energy, either to protect the batteries from overcharging or over-discharging, or to cover the power transfer needs that the ESS converter cannot support. According to the first term formulation, the energy manager aims to minimize the use of grid power if the system constraints allow.

Term 2 ($X_1 = 0$): when the constraints are fulfilled, the energy manager disconnects the hybrid system from the grid and lets the load be satisfied by the power mix between PV and ESS. When converging this term to 0, the energy manager can predict the ESS current during the cycling time, as this later depends only on the power balance between PV/ESS and load (ESS is not controllable anymore). Thanks to the predictable ESS current, the energy manager can keep tracking SOC evolution during the cycling time.

Optionally, Term 3 has been added to be active in grid-connected mode ($X_1 = 1$) when trying to satisfy the constraints. In cases where the power difference between load and PV/ESS is lower than a certain threshold, this term makes the energy manager switch to island mode to use the natural power flow to keep ESS within the tolerated operation zone instead of a forced mode (in grid-connected mode). This threshold is determined by the third weighting coefficient K_3.

2.4. GA optimization strategy

The cost function formulated in Eq. (4) is non-linear, which requires

Table 1
GA main optimization parameters.

Parameter	Value
Number of decision variables	2
Population	50
Generations	200
Function tolerance	1e−6
Constraints tolerance	1e−6

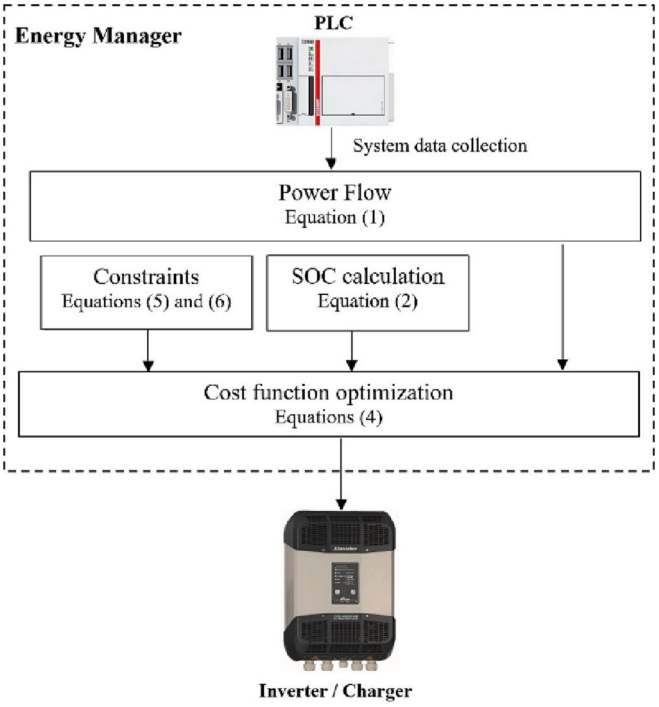

Fig. 2. Flowchart of the proposed optimization-based EMS.

a non-linear optimization method, which leads to the use of Genetic Algorithms (GA) strategy. Unlike other optimization methods, GA is a robust method capable of optimizing complex objective functions without having to know the objective function derivatives. GA is stochastic, easily parallelized and supports multi-objective optimization [24,25]. The GA optimization parameters are listed in Table 1. The rest of parameters are the ones set by default when using the predefined function in MATLAB.

2.5. Control procedure

During the initial test phase, the BAS PLC is to be bypassed

Table 2
INES hybrid system parameters.

Component	Subcomponent	Parameter	Value
PV system	PV module	Power at MPP	240 Wp
		Voltage at MPP	30.0 V
		Current at MPP	8.1 A
		Open circuit voltage	37.4 V
		Short circuit current	8.6 A
		Temperature coefficient	−0.46 %/K
		Module model	Bosch solar module c-Si M 60
	PV power plant	Number of modules	27
		Inclination	9 × 35° 18 × 30°
		Alignment	180° south
		Power	6.3 kWp
Batteries system	Battery cell	Voltage	4 V
		Nominal capacity	546 Ah
		Battery model	Rolls Battery 4CS17P
	Batteries bank	Number of cell in series	12
		Number of cells in parallel	1
		Power	4.5 kW
Programmable load	–	Nominal power	3.6 kW
		Load mode	Constant power
		Control mode	Remote
		Model	Chroma 63803

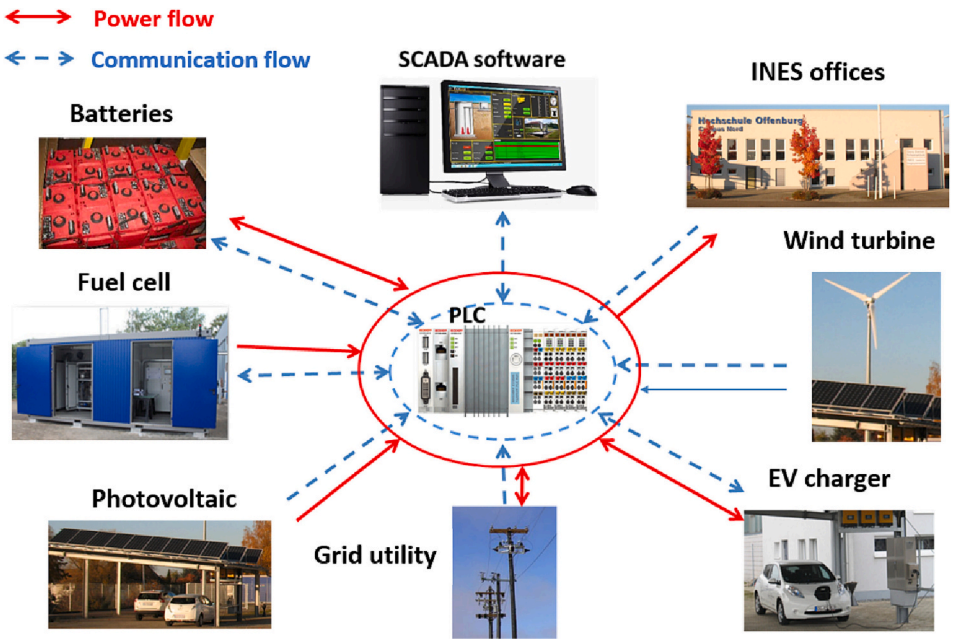

Fig. 3. INES smart grid system.

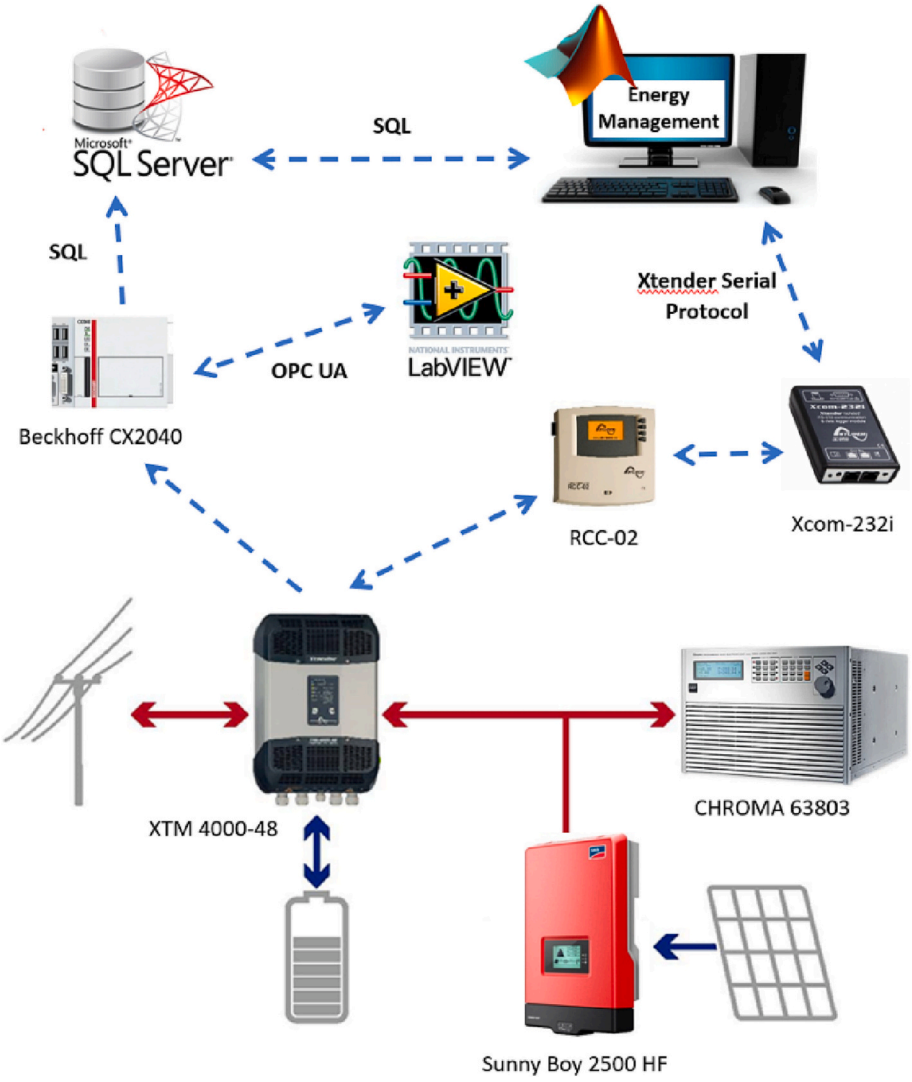

Fig. 4. Experimental setup.

temporarily, in which case the edge device (energy manager) controls, in real-time, the ESS inverter/charger directly. In this case, the serial RS-232 port is used as a physical connector. The communication is accomplished via a serial protocol provided by the inverter/charger manufacturer. Due to the relatively slow dynamic of the hybrid system, which is basically related to PV production and building power demand changes, the standard PC operation system (OS) is initially enough for carrying out EMS tasks. In industrial applications, where the system dynamic is fast or when real-time control is crucial, the standard OS is no longer valid, and the edge PC should be provided with a real-time OS (RTOS).

After retrieving PV, ESS, and load data from the local database, the SOC level at the end of the cycling time, can be predicted using Eq. (2). At this point, the GA optimization process can start. The optimization outcome is the control mode to be applied during the cycling time, either by controlling the ESS current or by connecting or disconnecting the grid utility. The target is to minimize the use of grid energy by driving optimally ESS while favoring island mode over grid-connected mode if the system constraints are respected. In island mode, ESS current is calculated using Eq. (7); negative values indicate charging currents, while positive values indicate discharging currents.

The controller ensures continuously that ESS SOC levels are maintained within the predefined maximum and minimum limits, SOC_{MAX} protects the batteries from overcharging and gasification, and assures enough capacity to recover any sudden PV power surplus. Unexpected PV peaks can be harmful if they are not stored or exported to the grid utility. SOC_{MIN} is kept at 50 % to avoid deep discharging scenarios and ensure a Depth Of Discharge (DOD) level below 50 %. Fig. 2 summarizes the schematic of the proposed control flowchart.

$$I_B = \frac{P_L - P_{PV}}{\eta_B \bullet V_B} \tag{7}$$

3. Experimental setup description

3.1. INES experimental setup description

In this section, more details about the implementation of the proposed EMS are given. The experimental system is a part of the smart grid prototype of the institute of energy systems technologies, commonly known as INES, at Offenburg University. General overview on INES smart grid subsystems is displayed in Fig. 3.

The test setup consists of three single phase STUDER XTM 4000-48 Xtender inverters/chargers in parallel to form a three-phase system. This three-phase inverter/charger is used to control the exchange of power between 4.5 kW lead-acid batteries and the emulated building microgrid. The inverter can also connect the whole local network to the grid or disconnect it to operate as an island microgrid. This operation is

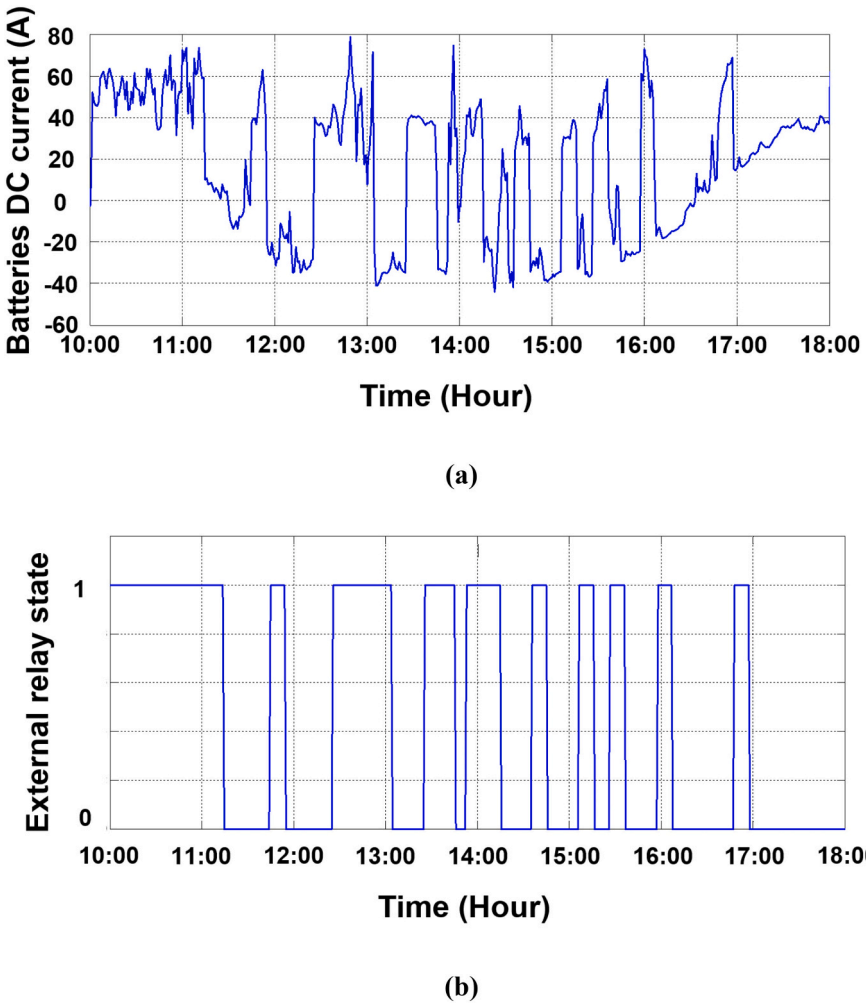

Fig. 5. Decision variables in clear-sky day test using optimization-based EMS: (a) ESS current, (b) grid relay state.

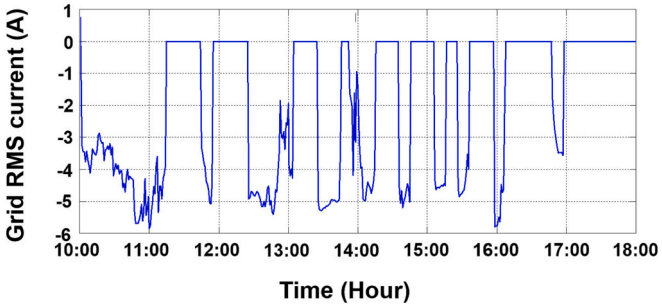

Fig. 6. Grid current variation in clear-sky day test using optimization-based EMS.

feasible by means of a relay called an "external relay". The 6.3 kWp PV system is connected to the AC bus via three Sunny Boy 2500 HF inverters, these inverters are controlled to supply the maximum available power to the microgrid. The different system parameters are listed in Table 2. The control cycling time is fixed at 10 min which fits the system dynamic; shorter control cycling times can lead to harmful operation of the ESS inverter/charger and the local energy network in general, while larger ones can make the controller unable to efficiently follow the system evolution as it will be mostly offline.

ESS status signals are measured permanently via the battery status processor (BSP) device, which offers real-time measurements of all battery parameters (SOC, voltage, current, and temperature). PV and load power data are other requested signals; they are collected via transmitters, treated by means of a Beckhoff CX2040 PLC, and stored, along with the local microgrid data, in a local database (Microsoft SQL Server). To simulate a residential building's power demand profile, three CHROMA 63803 programmable loads are connected to the local network to form a three-phase load system, and those loads are controlled remotely to follow a predefined profile. The PLC will also communicate with a Labview-based human machine interface (HMI) system via open platform communications united architecture (OPC UA) to offer data visualization in real time.

The system is initially designed in such a way that the ESS current setpoint is to be generated continuously by means of a PLC using a classical IF-THEN management code (rule-based). In this article, we prefer to use the GA-based optimization method, explained in Section 2, to generate an ESS setpoint for each cycling time. In this regard, a Windows-based PC is used as an edge device, and the optimization algorithm is coded using MATLAB as a high-level programming language. Real-time data is being retrieved from the database using SQL (structured query language) statements at each cycling time before running the optimization and building up the optimal control mode. During the test phase, instead of sending the ESS current setpoint to the PLC, the ESS inverter/charger is targeted instead, using a serial communication protocol. For this purpose, the Xcom-232i communication module is used. All system parameters, to be read or written, can be accessed in the Remote Control Center (RCC-02). The whole experimental prototype is presented in Fig. 4.

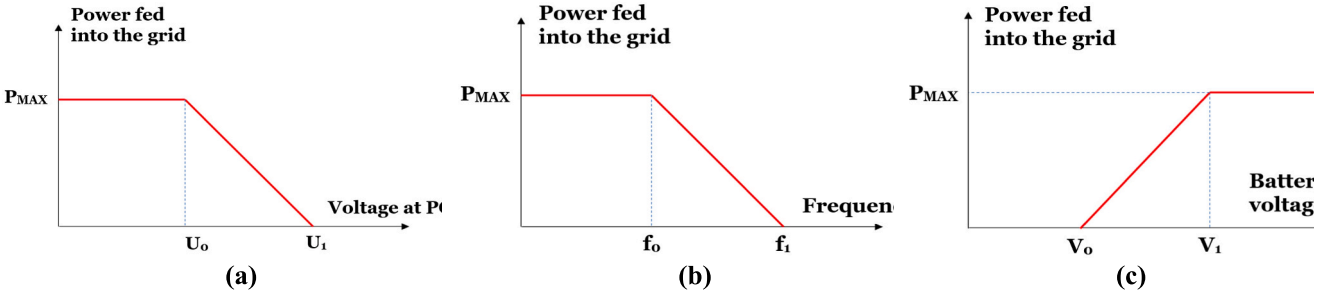

Fig. 7. Grid feeding internal control: (a) as a function of grid voltage at PCC (b) as a function of grid frequency (c) as a function of batteries voltage.

Table 3
Implemented voltage and frequency regulation parameters in grid feeding.

Parameter	Value	Description
U_0	230 V (ph-n)	The PCC voltage threshold in which the inverter starts the regulation process
U_1	240 V (ph-n)	The PCC voltage limit in which the inverter stops grid feeding
f_0	51 Hz	The frequency threshold in which the inverter starts the regulation process
f_1	53 Hz	The frequency limit in which the inverter stops grid feeding
V_0	46 V	The batteries voltage limit in which the inverter stops grid feeding
V_1	48 V	The batteries voltage threshold in which the inverter starts the regulation process

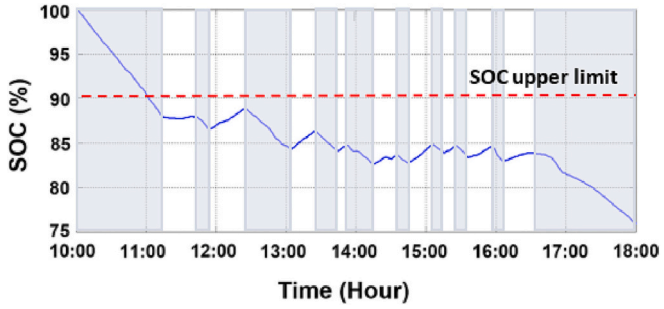

Fig. 8. ESS SOC variation in a clear-sky day test using optimization-based EMS.

3.2. PC – Xtender communication protocol

Xtender Serial Protocol is the communication method between Xcom-232i and the edge. This protocol is highly similar to Modbus RTU, in which the edge device, which is a personal computer (PC) in this case, acts as a master device. It consists of exchanging data frames composed of a header of 14 bytes followed by a variable number of data bytes and 2 bytes of checksum. To facilitate the implementation of the protocol, a Windows command-line tool provided by the manufacturer, combined with the MATLAB programming language, is used. As an example, to force the batteries to be charged under 12 A, the following command line statement is used in the Windows Command Prompt console:

```
>scom.exe --port=COM3 --verbose=3 write_property  src_addr=1
dst_addr=101 object_type=2 object_id=1138 property_id=5 format=FLOAT
value=12.0
```

where `write_property` is the "Write" function; `dst_addr=101` is the destination device address, in this case, 101 for Xtender; `object_id=1138` is the "charging current" parameter ID. `value=12.0` is the charging current value in Ampere.

To not oversize the content of this article, more information about the structure of the command lines and the Xtender Serial Protocol in general is to be referred to in the documentation section of the manufacturer's website.

The fact that Windows command-line statements can be formulated in MATLAB using the function "dos" dramatically facilitates the conception of any EMS policy. Sophisticated optimization algorithms can be simply called using predefined functions, such as "ga" for genetic algorithm optimization.

4. Results and discussions

In this section, the outcomes of the experimental tests using the setup

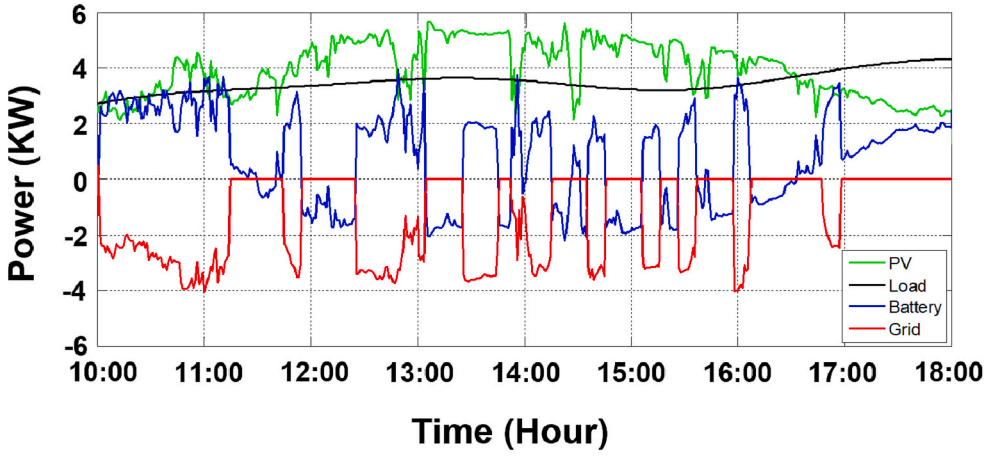

Fig. 9. Power share in clear-sky day test using optimization-based EMS.

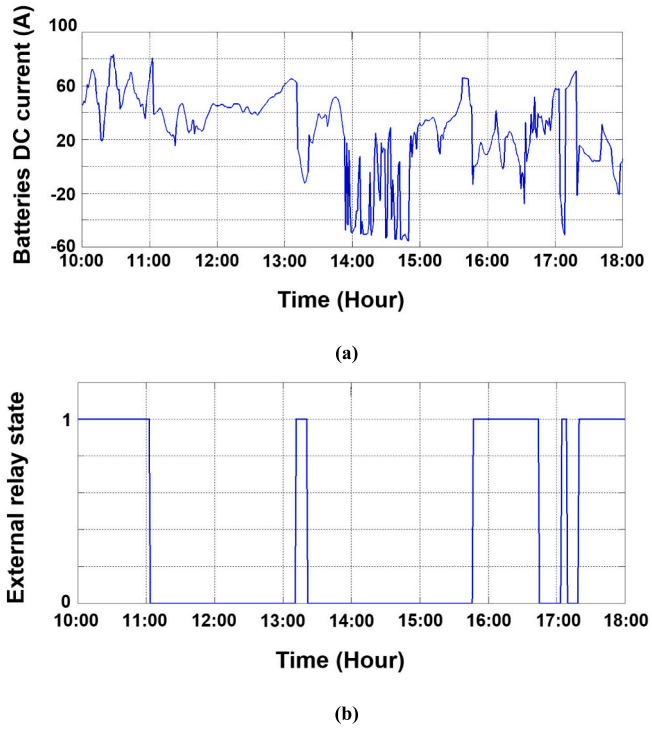

Fig. 10. Decision variables in partial-cloudy day test using optimization-based EMS: (a) ESS current, (b) grid relay state.

explained previously, are presented. Two main scenarios are considered: a clear-sky day, where the PV production rate is significant, and a partially cloudy day, where PV power is highly fluctuating. The purpose from the second test is to investigate the impact of high PV fluctuation on the robustness of the proposed EMS. The test is to be completed in 8 h, starting at 10:00. The system status signals are queried from the database each time cycle using the MATLAB database explorer. The selected upper and lower limits for ESS SOC are 90 % and 50 % respectively. The maximum allowed power for the ESS inverter/charger is fixed at 3.6 kW. The cost function weighting coefficients K_1, K_2 and K_3 are 1, 1 and 1e4, respectively, those values are reached after the "trial-and-error" method. The ESS charging and discharging conversion efficiency is assumed to be 97 %.

4.1. Clear-sky test

The optimized decision variables during the clear-sky test day are presented in Fig. 5. Before triggering the optimization process, the controller makes sure that the variables (ESS SOC/power) are initially within the acceptable predefined intervals, therefore, an ESS discharging process, through the grid utility, with a constant current is being performed during the first test hour (see Fig. 6). Appeared current fluctuations are caused by voltage and frequency regulation and batteries protection mechanisms. Fig. 7 shows the regulation strategy implemented in the inverter charger regarding the grid support and batteries safety functions, in which PCC is the point of common coupling of the inverter with the grid utility, while P_{MAX} is the power defined by EMS. The associated voltage/frequency regulation parameters are listed in Table 3. The controller can follow the evolution of SOC during the cycling time and keep it continuously within the allowed limits, as shown in Fig. 8. When the controller predicts a SOC upper constraint violation (90 %) at the end of the current cycling time, it operates the system in on-grid mode and feeds the extra power into the grid. When ESS SOC remains within the tolerant operation range, the system goes back to island mode. By doing so, the proposed EMS aims to charge ESS from the extra PV power only. ESS discharging periods are highlighted in Fig. 8 to show the ESS dynamic operation during the test. Fig. 9 shows the power share between different energy sources, storage, and loads. Since it consists of a sunny day test, the overall PV supplied energy was obviously higher than the load demand, which explains the frequent connection to the grid utility to feed extra power and keep ESS SOC below the upper limit.

4.2. Robustness test

The effectiveness of the proposed EMS approach will be determined by its robustness against high PV generation fluctuations. Supplied PV power depends highly on the insolation level; a partly cloudy day makes the generated PV power fluctuate, which may pose additional challenges to the energy manager's performance. During cycling time, PV modules may experience fast changes between cloudy and partially cloudy periods several times. This last case causes frequent PV power generation drops, which forces ESS to continuously cover the missed power. In some situations, ESS cannot fulfill this mission due to limited capacity in terms of power and SOC; this point is particularly critical in the case of island mode. Likely, the used ESS inverter/charger is equipped with an internal security feature that disconnects batteries in such a situation, whatever the external control mode.

The optimization decision variables in this case are displayed in Fig. 10. The PV power fluctuations are reflected directly on the ESS current in island mode (Fig. 10 (a)). The current fluctuations in grid-connected mode are due to the inverter grid support feature explained previously. In Fig. 10(b), we can clearly see that, in this particular test case, the island mode was applied for a longer time compared to the

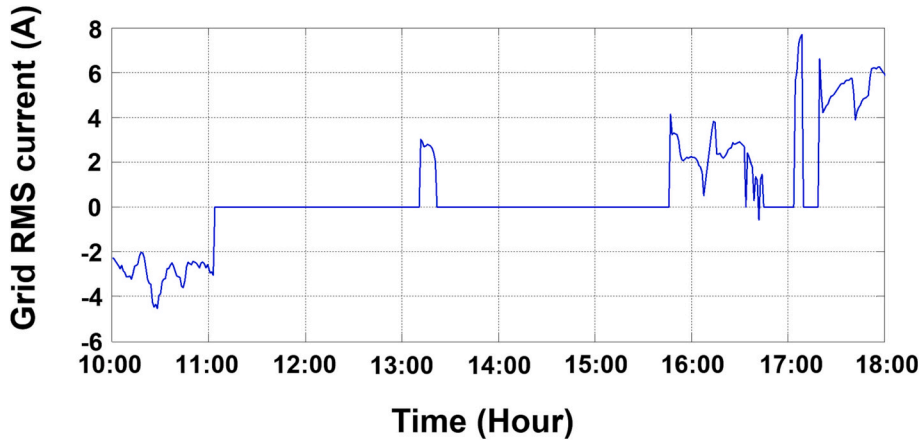

Fig. 11. Grid current variation in in partial-cloudy day test using optimization-based EMS.

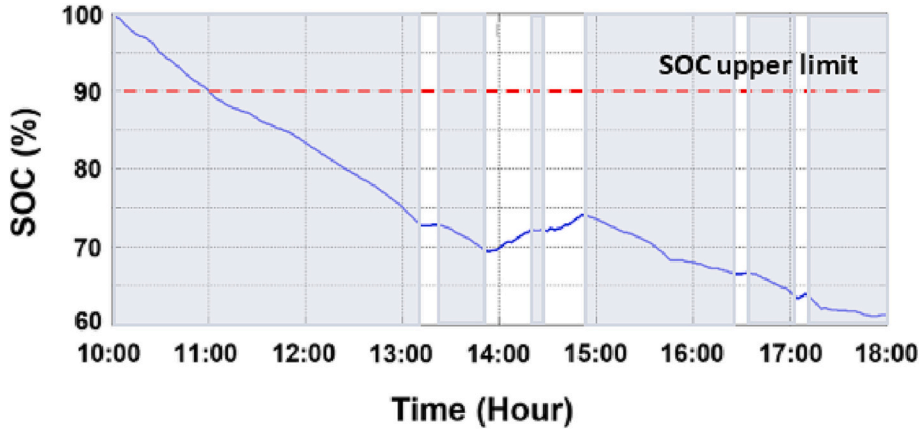

Fig. 12. ESS SOC variation in partial-cloudy day test using optimization-based EMS.

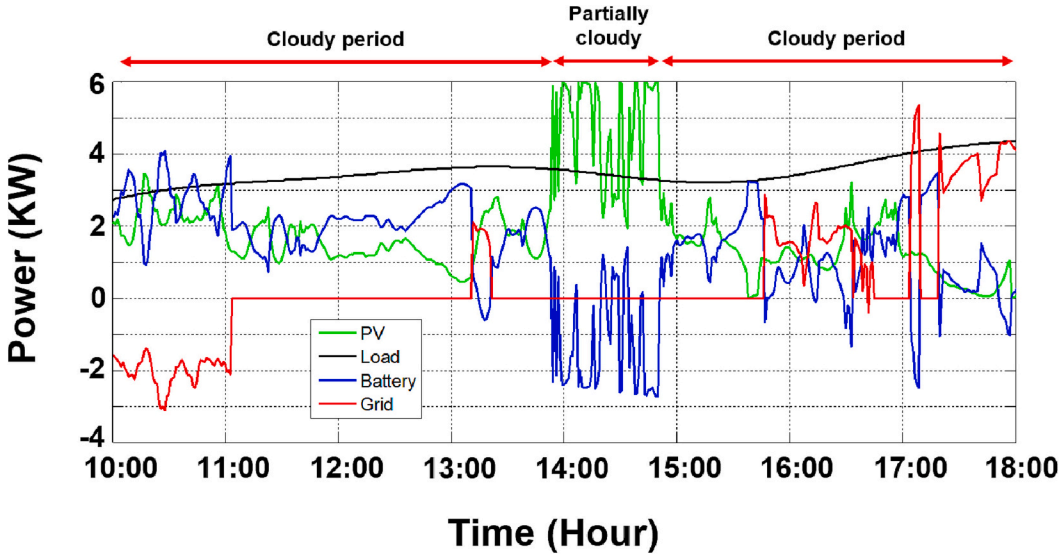

Fig. 13. Power share in partial-cloudy day test using optimization-based EMS.

previous test, which is explained by the ESS SOC that was running mostly within the accepted interval (see Fig. 12). However, the maximum allowed ESS power constraint was violated more than once, which explains the connection to the grid during the last 2 h of the test to sustain ESS with the imported power from the grid (see Fig. 11). The optimal power share is displayed in Fig. 13, which shows significantly reduced PV supplied energy compared to the first test. This scenario has led to a verified power balance in the microgrid, which explains the extended operation of island mode compared to the previous test. Apart from the case of ESS current fluctuations observed in island mode, the partially cloudy scenario had no significant effect on the EMS performance. However, those fluctuations in island mode can lead to battery performance degradation as a long-term impact if they are not dampened by a high dynamic ESS, such as ultracapacitors [26].

4.3. Baseline test (rule-based EMS)

Rule-based EMS is a simple method that offers a real-time evaluation of the energy system's performance using pre-defined conditions (rules). In this study, a rule-based ESS management system based on real-time evaluation of SOC is developed. It defines the operation mode of the hybrid system according to SOC level. The island mode is active only if the ESS constraints, formulated in Eqs. (5) and (6), are satisfied. The flowchart of the proposed rule-based EMS is shown in Fig. 14. Rule-based EMS is an efficient approach when it comes to cost-effective implementation. The rules are designed to focus mainly on ESS SOC variation. Operating ESS between predefined upper and lower limits offers various advantages: the lower limit protects ESS from deep undercharging scenarios, which increases the battery's life, and it also offers an energy backup in case any unexpected energy needs occur. The upper limit is put to protect the batteries from overcharging issues, such as corrosion on the positive plates and excessive temperatures. The upper limit also ensures the energy recovery capacity of any sudden extra PV supply, particularly in island mode. The control commands used to ensure the targeted performance are the same as those used in the previous optimization-based approach (external grid relay and ESS current). Rule-based methods can be performed online without requiring much computing time, which makes them suitable for real-time EMS.

Based on the testing day specifications, the control commands are defined as shown in Fig. 15. Accordingly, the system is moving continuously between island and grid-connected modes. Although the ESS current setpoint, defined by the energy management, is constant during the control cycling time (10 min), we can see in Fig. 15(a) current fluctuations. As stated earlier, this is due to the fact that the inverter/charger is designed to participate in the local grid voltage and frequency regulation by continuously adjusting the power fed to the grid. Nevertheless, those fluctuations are negligible compared to the constant

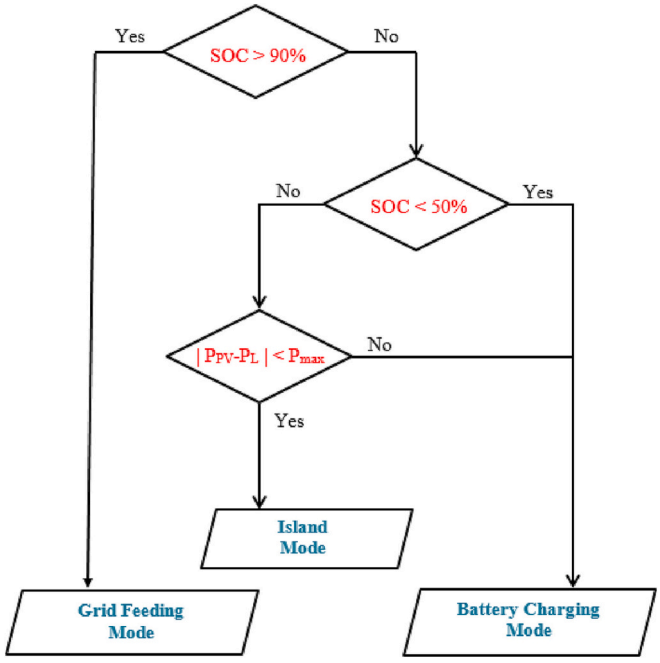

Fig. 14. Rule-based EMS flowchart.

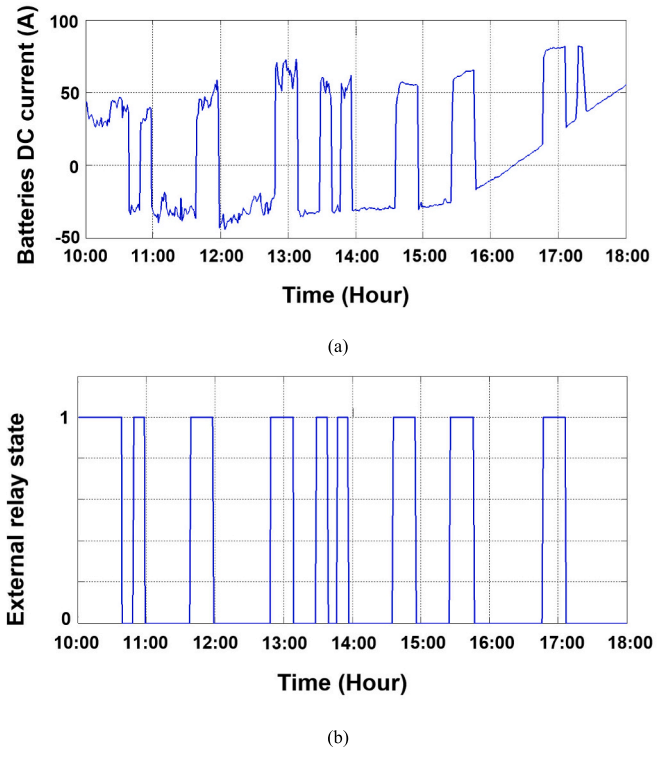

Fig. 15. Decision variables in a clear-sky day test using rule-based EMS: (a) ESS DC current, (b) grid relay.

setpoint defined by EMS.

As it was a sunny day, the amount of supplied PV energy was relatively larger compared to the energy demand (see Fig. 17), therefore, EMS aims to keep SOC below the upper limit by connecting a hybrid system to the grid to feed extra power. When SOC is turned back inside the tolerated zone, EMS operates the system in island mode again. During the test, ESS SOC crossed the upper limit several times, as shown in Fig. 16. This is due to the fact that EMS was totally offline during the cycling time. In this case, the control actions are being updated only after the end of each cycle. To protect the batteries from overcharging scenarios, EMS feeds extra power to the grid with different AC current levels, as shown in Fig. 18. Even though grid feeding current was defined constant (~6 A), the ESS inverter/charger adjusts the current setpoint for frequency/voltage regulation considerations, as they are prioritized over any EMS commands.

4.4. Comparison study

In this section, we would like to estimate the energy cost improvement using optimization-based EMS compared to the baseline method in the two different sunny days. Since the testing conditions were not perfectly matching for the two different EMS techniques, it is not trivial to quantify the difference in energy operation performance between them. Contrary to the power demand, which is generated by a programmable load device, it was obviously not possible to have the same supplied PV energy for all tests due to the different weather conditions. In this study, we could overcome this challenge by creating a common virtual operation scenario for both techniques. This reference scenario is when the produced PV energy is ideally matching the energy demand ($E_{PV}/E_{load} = 1$). The evaluation criteria is the energy exchanged with the grid. Accordingly, calculated values for both EMS techniques are listed in Table 4. As both testing scenarios are carried out on sunny days, supplied PV energies were considerable in such way the energy manager was often feeding back extra powers into the grid, which explains the negative values in Table 4. The table also shows 0.58 kWh more energy exported to the grid using optimization-based EMS compared to rule-based EMS during the seven testing hours, which represents an improvement of 6.23 %.

Regarding SOC control performance, Fig. 8. shows clearly that the optimization-based energy manager avoids driving ESS near the upper SOC limit in all different operation conditions, while Fig. 16 shows that the upper SOC limit has been violated few times using rule-based EMS, even though both strategies are carried out under comparable conditions. The reason is the ability of GA optimization to anticipate the power flow trend in the network and predict the system state at the end of the control horizon, therefore, it is possible to take command actions in advance to avoid SOC upper limit violations. Similarly, the proposed EMS performed better in terms of respecting the maximum exchanged power through the ESS inverter/charger (3.6 kW), while the rule-based approach violated this limit a few times during the test (see Figs. 9 and 17).

5. Conclusion

In this article, the implementation of advanced EMS into existing BAS using edge technology is investigated. Taking advantage of the available communication protocols of the low-level controllers and the high computing capability of the edge, sophisticated management algorithms can be implemented to optimize the energy use in the building's local network in real time. This article demonstrates the edge aptitude of significantly upgrading the data analytics capability of BAS by adding high-level hardware and software to the management layer. It has also been proven that, by applying GA-based optimization, to perform cyclically real-time control, it is possible to operate the hybrid energy system in island mode while ensuring system safety, consequently, renewable resources local self-share can be maximized. Furthermore, the robustness of the proposed management algorithm against rapid weather fluctuations has been verified.

Thanks to the short-horizon optimization, optimal operation setpoints have been periodically defined for each cycling time regardless of the optimization nonlinearity. As the main target is to minimize the imported energy from the grid or maximize the exported one, 6.23 % improvement in this context has been achieved for GA-optimization EMS in opposition to the classical rule-based EMS.

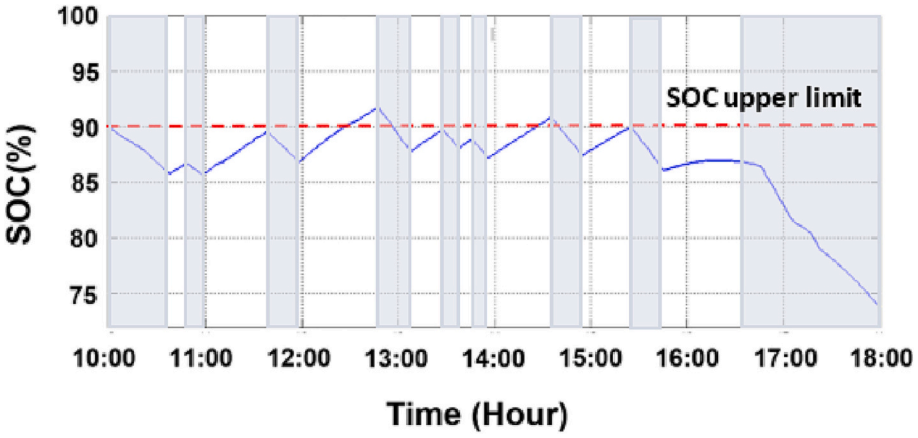

Fig. 16. ESS SOC variation in a clear-sky day test using rule-based EMS.

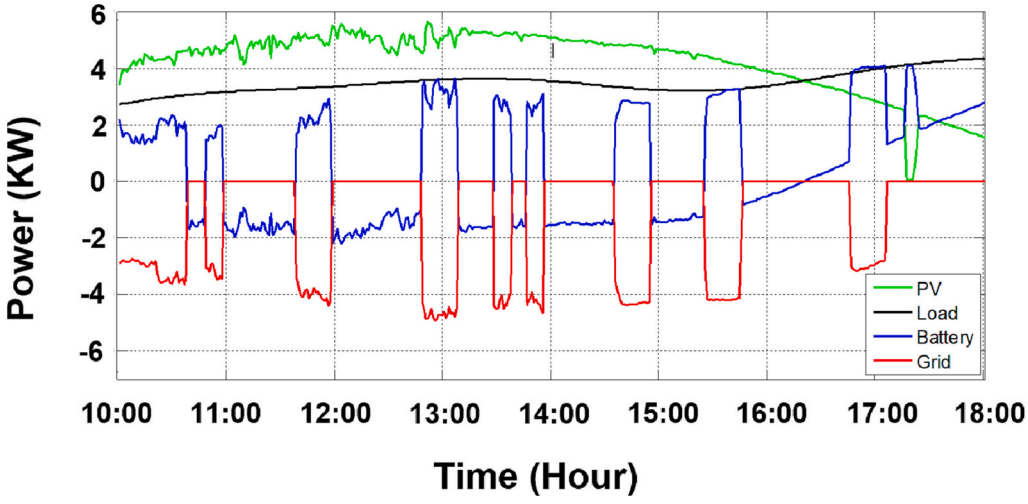

Fig. 17. Power share in clear-sky day test using rule-based EMS.

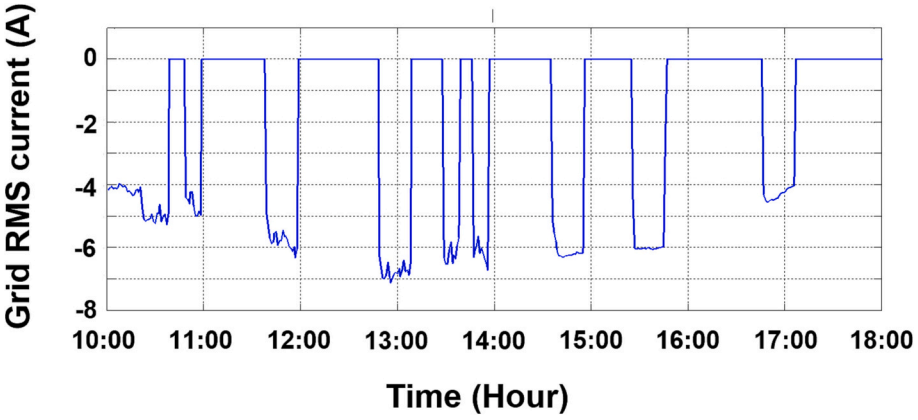

Fig. 18. Grid current variation in clear-sky day test using rule-based EMS.

Since the ESS safety is crucial in any EMS policy, the proposed strategy showed better performance compared to the classical rule-based approach when it comes to respecting the operation limits. As the power flow in the building's local network is predictable, the proposed EMS is capable of driving ESS within the tolerated margin in terms of SOC and exchanged power levels. Even though the energy manager is still offline during cycling time, GA optimization makes it possible to track the internal power flow direction and predict the ESS state at the end of the control horizon.

Declaration of competing interest

The authors declare the following financial interests/personal relationships which may be considered as potential competing interests:

Table 4
Energy cost comparison between rule-based and optimization-based EMSs.

EMS	Produced PV energy (E_{PV})	Consumed energy (E_{load})	Exchanged energy with the grid (E_{grid})	E_{PV}/E_{load}	Estimated exchanged energy with the grid when $E_{PV}/E_{load} = 1$
Rule-based	34.11 kWh	27.88 kWh	−10.65 kWh	1.22	−8.72
Optimization-based	31.9 kWh	27.88 kWh	−10.61 kWh	1.14	−9.30

Mustapha Habib reports financial support was provided by European Commission.

Data availability

No data was used for the research described in the article.

Acknowledgements

This research was funded by Algerian Ministry of Higher Education and Scientific Research in the framework of Programme National Exceptionnel (PNE). This research is also partially funded by EU H2020 programme under Grant Agreement No. 101036656.

References

[1] International Energy Agency, Energy Technology Perspectives 2012: Pathways to a Clean Energy System, 2012 (Paris (France)).
[2] Tracking Buildings, International Energy Agency, Paris, France, 2019. Available: https://www.iea.org/reports/tracking-buildings (Online).
[3] S. Saadon, L. Gaillard, S. Giroux-Julien, C. Menezo, Simulation study of a naturally-ventilated building integrated photovoltaic/thermal (BIPV/T) envelope, Renew. Energy 87 (2016) 517–531.
[4] W.L. Wang, Y.S. Liu, X.F. Wu, Y. Xu, W.Y. Yu, C.J. Zhao, Y.B. Zhong, Environmental assessments and economic performance of BAPV and BIPV systems in Shanghai, Energy Build. 130 (2016) 98–106.
[5] Waqar A. Qureshi, Nirmal-Kumar C. Nair, Mohammad M. Farid, Impact of energy storage in buildings on electricity demand side management, Energy Convers. Manag. 52 (2011) 2110–2120.
[6] Shu Tang, Dennis R. Shelden, Charles M. Eastman, Pardis Pishdad-Bozorgi, Xinghua Gao, BIM assisted Building Automation System information exchange using BACnet and IFC, Autom. Constr. 110 (2020), 103049.
[7] R. Yang, L. Wang, Multi-objective optimization for decision-making of energy and comfort management in building automation and control, Sustain. Cities Soc. 2 (2012) 1–7, https://doi.org/10.1016/j.scs.2011.09.001.
[8] M. Dastbaz, C. Gorse, A. Moncaster, Building Information Modelling, Building Performance, Design and Smart Construction, Springer Nature Switzerland AG, Cham, 2017.
[9] W. Tushar, et al., Internet of things for green building management: disruptive innovations through low-cost sensor technology and artificial intelligence, IEEE Signal Process. Mag. 35 (5) (2018) 100–110, https://doi.org/10.1109/MSP.2018.2842096.
[10] W. Xu, et al., The design, implementation, and deployment of a smart lighting system for smart buildings, IEEE Internet Things J. 6 (4) (2019) 7266–7281, https://doi.org/10.1109/JIOT.2019.2915952.
[11] S.H. Khajavi, N.H. Motlagh, A. Jaribion, L.C. Werner, J. Holmström, Digital twin: Vision, benefits, boundaries, and creation for buildings, IEEE Access 7 (Oct. 2019) 147,406–147,419, https://doi.org/10.1109/ACCESS.2019.2946515.
[12] E. Png, S. Srinivasan, K. Bekiroglu, J. Chaoyang, R. Su, K. Poolla, An internet of things upgrade for smart and scalable heating, ventilation and air-conditioning control in commercial buildings, Appl. Energy 239 (Apr. 2019) 408–424, https://doi.org/10.1016/j.apenergy.2019.01.229.
[13] Y. Liu, C. Yang, L. Jiang, S. Xie, Y. Zhang, Intelligent edge computing for IoT-based energy management in smart cities, IEEE Netw. 33 (2) (2019) 111–117, https://doi.org/10.1109/MNET.2019.1800254.
[14] Zhishu Shen, Jiong Jin, Tiehua Zhang, Atsushi Tagami, Teruo Higashino, Qing-Long Han, Data-driven edge computing: a fabric for intelligent building energy management systems, IEEE Ind. Electron. Mag. 16 (2) (June 2022), https://doi.org/10.1109/MIE.2021.3120235.
[15] X. Wang, Y. Han, V.C.M. Leung, D. Niyato, X. Yan, X. Chen, Convergence of edge computing and deep learning: a comprehensive survey, IEEE Commun. Surveys Tuts. 22 (2) (2020) 869–904, https://doi.org/10.1109/COMST.2020.2970550.
[16] Balint Hartmann, Istvan Taczi, Attila Talamon, Istvan Vokony, Island mode operation in intelligent microgrid—extensive analysis of a case study, Int. Trans. Electr. Energy Syst. 31 (2021), e12950, https://doi.org/10.1002/2050-7038.12950.
[17] Ghazanfar Shahgholian, A brief review on microgrids: operation, applications, modeling, and control, Int. Trans. Electr. Energy Syst. 31 (2021), e12885, https://doi.org/10.1002/2050-7038.12885.
[18] Jürgen Marchgraber, Wolfgang Gawlik, Investigation of black-starting and islanding capabilities of a battery energy storage system supplying a microgrid consisting of wind turbines, Impedance and Motor Loads Energies 13 (2020) 5170, https://doi.org/10.3390/en13195170.
[19] Mustapha Habib, Ahmed Amine Ladjici, Farid Khoucha, Frequency control in off-grid hybrid diesel/PV/battery power system, in: International Conference on Electrical Engineering. Algiers, Algeria, December 2015.
[20] SMA, Design of off-grid systems with Sunny Island 4.4M/6.0H/8.0H devices, Available online: https://files.sma.de/downloads/Designing-OffGridSystem-PL-en-24.pdf, 2020. (Accessed 23 June 2020).
[21] Mustapha Habib, Ahmed Amine Ladjici, Abdelghani Harrag, Microgrid management using hybrid inverter fuzzy-based control, Neural Comput. & Applic. 32 (2020) 9093–9111.
[22] Mustapha Habib, Ahmed Amine Ladjici, Elmar Bollin, Michael Schmidt, One-day ahead predictive management ofbuilding hybrid power system improvingenergy cost and batteries lifetime, IET Renew. Power Gener. 13 Iss. 3 (2019) 482–490.
[23] Tatiane Carolyne Carneiro, Paulo Cesar Marques, Heron de Carvalho, Alves dos Santos, Marcello Anderson Ferreira Batista Lima, Arthur Plinio, de Souza Braga., Review on photovoltaic power and solar resource forecasting: current status and trends, J. Solar Energy Eng. 144 (Feb 2022), 010801-1.
[24] Stefano Leonori, Maurizio Paschero, Fabio Massimo Frattale Mascioli, Antonello Rizzi, Optimization strategies for Microgrid energy management systems by Genetic Algorithms, Appl. Soft Comput. J. 86 (2020), 105903.
[25] Ramin Torkan, Adrian Ilinca, Milad Ghorbanzadeh, A genetic algorithm optimization approach for smart energy management of microgrids, Renew. Energy 197 (2022) 852–863.
[26] Ahmad M.A. Malkawi, Luiz A.C. Lopes, Improved dynamic voltage regulation in a droop controlled DC nanogrid employing independently controlled battery and supercapacitor units, Appl. Sci. 8 (2018) 1525, https://doi.org/10.3390/app8091525.